11

Solution Guide and Solutions of the Problems

11.1 Problems of Chapter 2

Problem 2.1

a) We find from Table B.1 with linear interpolation $\rho_\infty = 1.64{\cdot}10^{-5}$ kg/m^3 and $T_\infty = 196.7$ K. From $q_\infty = 0.5\rho_\infty v_\infty^2$ we obtain $v_\infty = 7,648.1$ m/s. The speed of sound is $a_\infty = (\gamma\, R\, T_\infty)^{0.5}$. With $R = 287.06$ m^2/s^{2}K, Table C.1, and $\gamma = 1.4$, we get $a_\infty = 281.1$ m/s and $M_\infty = 27.2$.

b) We find from Table B.1 $\rho_\infty = 9.89{\cdot}10^{-5}$ kg/m^3 and $T_\infty = 222.3$ K and obtain $v_\infty = 6,198.6$ m/s, $a = 298.9$ m/s and $M_\infty = 20.7$.

Problem 2.2

From eq. (9.2) we find $T_{ra} = 1,085.8$ K.

Problem 2.3

At 70 km altitude we have $\rho_\infty = 8.283 \cdot 10^{-5}$ kg/m^3, Table B.1. With eq. (10.76) we find $q_{gw} = 411.7$ kW/m^2 and from eq. (9.2) $T_{ra} = 1,709.6$ K. This temperature is within the limits. The nose cone of the Orbiter is made of reinforced carbon-carbon (RCC). This material performs up to approximately 2,000 K [1]. We observe moreover, that the radiation-adiabatic temperature is larger than the actual temperature due to heat conduction into and within the nose cap material, see for example Sub-Section 8.4.3.

Problem 2.4

Proceed as with Problem 2.3. The temperature is above the limit.

Problem 2.5

a) Using the equations

$$V_{circ} = [(R_E + H)g(H)]^{1/2},$$
$$V_E = \omega(R_E + H),$$
$$g = g_0 \left(\frac{R_E}{R_E + H}\right)^2,$$

and setting $V_{circ} = V_E$, we find $H = 35.8096 \cdot 10^6$ m.

b) By applying the eqs. (2.55) we use

$$V_{|g}^0 = 0 \text{ m/s},$$

and by eqs. (2.56)

$$V_{|g}^g = V_{circ} = 3,076.5 \text{ m/s}.$$

11.2 Problems of Chapter 3

Problem 3.1

We find from Table B.1 for each altitude the temperature T_∞ and the density ρ_∞. With the speed of sound $a_\infty = (\gamma R T_\infty)^{0.5}$, $R = 287.06$ m^2/s^{2}K, Table C.1, and $\gamma = 1.4$, we obtain the velocities v_∞. Finally with $q_\infty = 0.5 v_\infty^2$ we obtain 1) $q_\infty = 0.51$ kPa, 2) $q_\infty = 1.79$ kPa, 3) $q_\infty = 3.79$ kPa, 4) $q_\infty = 5.92$ kPa, 5) $q_\infty = 7.48$ kPa, 6) $q_\infty = 9.69$ kPa. At these altitudes the dynamic pressures are below the maximum dynamic pressure $q_\infty \approx 14$ kPa.

Problem 3.2

The total enthalpy is at the ambient temperatures of the atmosphere T_∞

$$h_t = h_\infty + \frac{1}{2} v_\infty^2 = \frac{\gamma}{\gamma - 1} R T_\infty + \frac{1}{2} v_\infty^2.$$

We find with the data from Problem 3.1: 1) $h_t = 0.199 \cdot 10^6 + 27.819 \cdot 10^6 = 28.019 \cdot 10^6$ m^2/s^2, $\Delta k = 99.3$ per cent, 2) $h_t = 21.771 \cdot 10^6$ m^2/s^2, $\Delta k = 99$ per cent, 3) $h_t = 12.483 \cdot 10^6$ m^2/s^2, $\Delta k = 98$ per cent, 4) $h_t = 6.042 \cdot 10^6$ m^2/s^2, $\Delta k = 95.5$ per cent, 5) $h_t = 2.123 \cdot 10^6$ m^2/s^2, $\Delta k = 88.1$ per cent, 6) $h_t = 0.753 \cdot 10^6$ m^2/s^2, $\Delta k = 69.8$ per cent.

Problem 3.3

From eq. (2.8) we find for small and constant γ:

$$m = \frac{L}{g - (v_\infty^2/R_\infty)}.$$

The earth acceleration at $H = 80$ km altitude is, Section C.1: $g = 9.565\ \mathrm{m/s^2}$. The radius $R_\infty = R_E + H$ is $6.458 \cdot 10^6$ m. With $q_\infty = 0.513$ kPa and $v_\infty = 7,459.1$ m/s, see Problem 3.1, we get a) $m = 118,709$ kg, b) $v_\infty^2/R_\infty = 8.61\ \mathrm{m/s^2} \mathrel{\widehat{=}} 90$ per cent, c) $W = 1,164,144$ N.

Problem 3.4

From eq. (2.8) we find for small and constant γ:

$$v_\infty = \sqrt{\frac{g}{\dfrac{C_L A_{ref} \rho_\infty}{2m} + \dfrac{1}{R_\infty}}}.$$

At 80 km altitude we have $\rho_\infty = 1.846 \cdot 10^{-5}\ \mathrm{kg/m^3}$, Table B.1. With $R_\infty = 6.458 \cdot 10^6$ m, we find $v_\infty = 7,570$ m/s and $M_\infty = 26.8$.

Problem 3.5

The dynamic pressure at $M_\infty = 24$, $H_\infty = 70$ km is $q_\infty = 2.105$ kPa. The force acting on the boattailing surface is $F_N = \Delta c_{p_w} A_{bt} q_\infty$. The delta force is $\Delta F_N = 157,100 - 179,960 = -22,860$ N and the delta normal force coefficient $\Delta C_N = \Delta F_N/(q_\infty A_{ref}) = -0.0434$. The delta moment is $\Delta M = -\Delta F_N(0.91 - 0.665)L_{ref} = 194,68$ Nm and the delta pitching moment $\Delta C_m = \Delta M/(\overline{c} A_{ref} q_\infty) = 0.0307$.

Problem 3.6

a) With the help of eq. (7.23) we obtain $C_N = 1.205$ and $C_X = 0.0608$.

b) The plan area of the Orbiter is $A_{plan} = 361.3\ \mathrm{m^2}$. Subtracting the boattailing area $A_{bt} = 135.7\ \mathrm{m^2}$, we find what we call the main surface to $A_{ms} = 225.6\ \mathrm{m^2}$. With the approximate normal force coefficient

$$C_N \approx \frac{c_{p_{w,ms}} A_{ms} + c_{p_{w,bt}} A_{bt}}{A_{ref}},$$

we obtain, case 2.a: $C_N = 1.145$ and case 2.c: $C_N = 1.093$.

c) C_X is much smaller than C_N, because the surface pressure at the windward side acts predominantly in normal force direction, Fig. 3.37. C_N of case 2.c is

smaller than that of case 2.a because of the Mach number and high temperature real gas effects. The level of these coefficients is smaller than that found by the transformation of the data base coefficients, because in this simple approximation the higher c_{p_w} at the nose part of the vehicle was not taken into account.

Problem 3.7

The dynamic pressure at $M_\infty = 22.1$ and $H = 70$ km is $q_\infty = 1.79$ kPa.

a) We assume, that the stagnation point streamline penetrates the bow shock surface orthogonally. Then we have $c_{p_{w,perfect,stag}} = 1.8394$.

b) The force on the stagnation point area is $\Delta F_N = (c_{p_{w,real,stag}} - c_{p_{w,perfect,stag}}) q_\infty \Delta A_{nose} = 180.07$ N. $\Delta C_N = \Delta F_N / (q_\infty A_{ref}) = 4.02 \cdot 10^{-4}$.

c) $\Delta M = \Delta F_N x_l = 3,835.6$ Nm, $\Delta C_M = (\Delta F_N x_l)/(q_\infty A_{ref} \overline{c}) = 7.1 \cdot 10^{-4}$.

Problem 3.8

a) The boattailing force is $F_{bt} = 153{,}028.9$ N. The normal force is $F_{bt} = N = 539{,}043.4$ N and hence $F_{ms} = 386{,}014.5$ N. From eq. (3.10) we get:

$$x_{ms} = \frac{F_{res}\, x_{cp} - F_{bt}\, x_{bt}}{F_{ms}}.$$

The location of x_{cp} is found with the help of the moment and the normal force coefficient: $\triangle x = \text{-}\, M/N = \text{-}\, C_M\, \overline{c}/C_N = 0.41034$ and $x_{cp} = x_{cog} + \triangle x = 21.71$ m. With $x_{bt} = 29.82$ m we get finally $x_{ms} = 18.4936$ m.

b) The boattailing force is now $F'_{bt} = 133,600$ N. With eq. (3.11) we have

$$x'_{cp} = \frac{x_{ms} + x_{bt} \dfrac{F'_{bt}}{F_{ms}}}{1 + \dfrac{F'_{bt}}{F_{ms}}},$$

and $x'_{cp} = 21.41$ m.

c) The forward shift of the center of pressure is $|\Delta\, x_{cp}| \approx 0.30$ m.

11.3 Problems of Chapter 4

Problem 4.1

We employ the flat surface relations given in Section 10.4. The recovery temperature is

$$T_r = T_e(1 + r\frac{\gamma - 1}{2}M_e^2).$$

The viscosity is determined with eq. (10.61) for $T \gtrapprox 200$ K. We find $T_{r,lam} = 2,070$ K, $T_{r,turb} = 2,150$ K, $T^*_{r,lam} = 803.03$ K, $T^*_{r,turb} = 1,016.84$ K. Because all temperatures are above $T = 200$ K, eq. (10.99) can be written as

$$c_f = 2\,C\,x^{-n}\left(\frac{T_e}{T^*}\right)^{1-n(1+\omega)}(Re_e^u)^{-n}\,.$$

The result must be re-normalized with the dynamic pressure q_∞. We obtain a) $c_{f,lam} = 1.10 \cdot 10^{-4}$, $c_{f,turb} = 1.61 \cdot 10^{-3}$.

The relation for the heat flux in the gas at the wall, eq. (10.100), is used in the form:

$$q_{gw} = C\,x^{-n}\,k_e\,Pr^{1/3}(T_r - T_w)\left(\frac{T_e}{T^*}\right)^{1-n(1+\omega)}(Re_e^u)^{1-n}\,.$$

We obtain b) $q_{gw,lam} = 2.69\,\mathrm{kW/m^2}$, $q_{gw,turb} = 31.73\,\mathrm{kW/m^2}$. The agreement with the data in Fig. 4.8 is quite good.

Problem 4.2

We write eq. (10.88) in the form

$$\delta = C\frac{x^{1-n}}{(Re_e^u)^n}\left(\frac{T^*}{T_e}\right)^{n\,\omega},$$

and obtain $\delta_{lam} = 0.043$ m (with the alternative relation for δ_{lam}, eq. (10.89), the thickness is smaller). With the other relations from Sub-Section 10.4.2 we find $\delta_{1,lam} = 0.022$ m, $\delta_{turb} = 0.66$ m, $\delta_{1,turb} = 0.187$ m, $\delta_{vs} = 0.002$ m.

Problem 4.3

We obtain $c_{f,lam} = 0.57 \cdot 10^{-4}$, $c_{f,turb} = 0.58 \cdot 10^{-3}$, $q_{gw,lam} = 1.35\ \mathrm{kW/m^2}$, $q_{gw,turb} = 11.02\ \mathrm{kW/m^2}$, $\delta_{lam} = 0.078$ m, $\delta_{1,lam} = 0.043$ m, $\delta_{turb} = 0.84$ m, $\delta_{1,turb} = 0.255$ m, $\delta_{vs} = 0.005$ m.

The skin-friction coefficients and the heat flux in the gas at the wall are smaller, the thicknesses are larger. The latter reflect directly the smaller Reynolds number, which is the flight Reynolds number, whereas the former are influenced by the changed flow parameters at the lower side of the forebody.

Problem 4.4

We find $c_{f,turb} = 0.612 \cdot 10^{-3}$, $q_{gw,turb} = 0.152\ \mathrm{kW/m^2}$, $\delta_{turb} = 0.54$ m, $\delta_{1,turb} = 0.128$ m.

a) The heat flux in the gas at the wall is small because of the chosen large wall temperature.

b) The boundary layer thicknesses are smaller than before, mainly because of the much larger unit Reynolds number.

c) The skin friction increases.

Problem 4.5

From eq. (4.8) we obtain for small angles $\overline{\alpha}$ and $\gamma = 1.4$

$$\theta|_{M_\infty \to \infty, \overline{\alpha} \ll 90^\circ} = \frac{\gamma - 1}{\gamma + 1} = 0.1667.$$

Problem 4.6

Newton's theory gives $C_L = 2 \sin^2 \overline{\alpha} \cos \overline{\alpha}$ and $C_D = 2 \sin^3 \overline{\alpha}$.

We find for $\overline{\alpha} = 9.4^\circ$: $C_L = 0.0526$, $C_D = 0.00871$, for $\overline{\alpha} = 8.4^\circ$: $C_L = 0.0422$, $C_D = 0.00623$, and for $\overline{\alpha} = 10.4^\circ$: $C_L = 0.0641$, $C_D = 0.0118$.

The changes are for $\overline{\alpha} = 8.4^\circ$: $\Delta C_L = -19.8$ percent, $\Delta C_D = -28.5$ percent, and for $\overline{\alpha} = 10.4^\circ$: $\Delta C_L = +21.9$ percent, $\Delta C_D = +35.5$ percent.

The changes are, in view of Fig. 4.44, very large. This means that, in order to arrive at a reliable conclusion, the performance changes of the whole vehicle must be considered, see the remarks at the end of Sub-Section 4.5.4.

Problem 4.7

In spherical coordinates rot $\underline{v}$ reads:

$$\mathrm{rot}\underline{v} = \begin{pmatrix} \frac{1}{r}\frac{\partial v_\varphi}{\partial \theta} - \frac{1}{r \sin\theta}\frac{\partial v_\theta}{\partial \varphi} + \frac{\cot\theta}{r} v_\varphi \\ \frac{1}{r \sin\theta}\frac{\partial v_r}{\partial \varphi} - \frac{\partial v_\varphi}{\partial r} - \frac{1}{r} v_\varphi \\ \frac{\partial v_\theta}{\partial r} - \frac{1}{r}\frac{\partial v_r}{\partial \theta} + \frac{1}{r} v_\theta \end{pmatrix} = 0.$$

For conical and axisymmetric flows we have $\frac{\partial}{\partial r} = 0$, $\frac{\partial}{\partial \varphi} = 0$, $v_\varphi = 0$ and from the third component of rot $\underline{v}$ we find $v_\theta = \frac{\partial v_r}{\partial \theta}$.

Problem 4.8

With $L_{ref} = 80$ m, we have $\Delta x = x_N - x_{cp} = 40$ cm. From eqs. 7.18 and 7.23 we find with the 1 percent condition:

$$\begin{aligned} \Delta z|^{\alpha=0^\circ} &= 1.60\,\mathrm{cm}, \\ \Delta z|^{\alpha=3^\circ} &= 2.40\,\mathrm{cm}, \\ \Delta z|^{\alpha=10^\circ} &= 2.88\,\mathrm{cm}. \end{aligned}$$

11.4 Problems of Chapter 5

Problem 5.1

1. The coefficient of surface pressure is $c_{p_w} = 2\sin^2(\alpha + \theta)$.
2. The unit-surface force F_{aero} acting on a surface element $d\,S$ is only a pressure force and hence $F_{aero} = p_w = c_{p_w} q_\infty$ acts normal to the (windward) surface element. The resultant force R, also acting normal to the windward surface $A = w\,L/\cos\theta$, is $R = c_{p_w} q_\infty A = c_{p_w} q_\infty\, 0.1\, L^2/\cos\theta$ and its coefficient $C_R = R/(q_\infty A_{ref}) = c_{p_w}/\cos\theta$.
3. The normal force is $Z = R\cos\theta$, the axial force is $X = R\sin\theta$, and their coefficients are $C_Z = c_{p_w}$ and $C_X = c_{p_w}\tan\theta$.
4. The pitching moment is $M = -RL/(2\cos\theta)$ and its coefficient $C_m = M/(q_\infty\, A_{ref}\, L_{ref}) = -c_{p_w}/\cos^2\theta$.
5. The surface element dS is connected to dx by $dS = w\,dx/\cos\theta$ and to dz by $dS = -w\,dz/\sin\theta$. The components of the unit-surface force F_{aero} are $F_{x,aero} = F_{aero}\sin\theta$ and $F_{z,aero} = F_{aero}\cos\theta$.
6. The moment M is split according to eq. (7.4). We find with eqs. (7.9) $C_m|_0^x = -(w/(q_\infty A_{ref} L_{ref}))\int_0^L c_{p_w} q_\infty x dx = -c_{p_w}$ and $C_m|_0^z = -(w/(q_\infty A_{ref} L_{ref}))\int_{-L\tan\theta}^0 c_{p_w} q_\infty z dz = -c_{p_w}\tan^2\theta$.
7. The coordinates of the center-of-pressure are finally with eqs. (7.5) and (7.7) $x_{cp} = L_{ref} C_m|_0^x / C_Z = -0.5L$ and $z_{cp} = -L_{ref} C_m|_0^z / C_X = +0.5L\tan\theta$.
8. The x-coordinate of the center-of-gravity for trim is like eq. (7.11) $x_{cog} = x_{cp} - (C_X/C_Z) z_{cp}$, Fig. 7.5.

Problem 5.2

The pressure coefficient on the windward side comes to

$$c_p^w = 2\sin^2(\phi_w + \alpha),$$

and on the leeward side to

$$c_p^l = 2\sin^2(\phi_w - \alpha).$$

The lift coefficient is given by

$$\begin{aligned} C_L &= C_L^w - C_L^l = \\ &= 2\sin^2(\phi_w + \alpha)\cos(\phi_w + \alpha) - 2\sin^2(\phi_w - \alpha)\cos(\phi_w - \alpha). \end{aligned}$$

a) $\phi_w = 45°$, $\alpha = 45° \Longrightarrow C_L = 0$.

b) The function $C_L(\phi_w, \alpha)$ possesses a turning point in $\alpha = 0°$ with:

$$\frac{dC_L}{d\alpha} = -2\left(\sin^3(\phi_w+\alpha)+\sin^3(\phi_w-\alpha)\right)+$$
$$+4\left(\sin(\phi_w+\alpha)\cos^2(\phi_w+\alpha)+\sin(\phi_w-\alpha)\cos^2(\phi_w-\alpha)\right)=$$
$$=0,$$

and from $dC_L/d\alpha|_{\alpha=0}=0$ one finds

$$\phi_w = \arcsin\sqrt{\frac{2}{3}} = 54.732^\circ.$$

With that the inequality holds

$$\sin^2(\arcsin\sqrt{\frac{2}{3}}+\alpha)\cos(\arcsin\sqrt{\frac{2}{3}}+\alpha) <$$
$$< \sin^2(\arcsin\sqrt{\frac{2}{3}}-\alpha)\cos(\arcsin\sqrt{\frac{2}{3}}-\alpha)$$

for any $\alpha \le 45^\circ$, which means that C_L is negative.

Problem 5.3

From eq. 7.2 we have

$$L_{ref}\ C_{m(1)} - (x_{(1)}-x_{cp})C_z + (z_{(1)}-z_{cp})C_x = 0,$$
$$L_{ref}\ C_{m(0)} - (x_{(0)}-x_{cp})C_z + (z_{(0)}-z_{cp})C_x = 0,$$

and

$$L_{ref}\, C_{m(1)} = L_{ref}\, C_{m(0)} + (x_{(1)}-x_{(0)})\, C_z - (z_{(1)}-z_{(0)})\, C_x.$$

With $C_{m(0)}=0.13$, $C_x=1.45$, $C_z=0.42$ we find

$$C_{m(1)} = -0.0539.$$

Problem 5.4

For the quarter circle we find, Fig. 11.1

$$F_x|^{circ} = q_\infty 2r\int_0^{\pi/2}\cos^2(\varphi-\alpha)\sin(\frac{\pi}{2}+\varphi)\ d\varphi$$
$$= q_\infty 2r\left(\frac{1}{3}+\frac{1}{3}\cos\alpha\ (\cos\alpha+2\sin\alpha)\right)$$
$$= q_\infty A_{ref} C_x|^{circ},$$

$$
\begin{aligned}
F_z|^{circ} &= q_\infty 2r \int_0^{\pi/2} \cos^2(\varphi-\alpha)\sin\varphi \, d\varphi \\
&= q_\infty 2r \left(\frac{1}{3} + \frac{1}{3}\sin\alpha \, (\sin\alpha + 2\cos\alpha) \right) \\
&= q_\infty A_{ref} C_z|^{circ},
\end{aligned}
$$

$$
\begin{aligned}
C_m|_o^{x,circ} &= -\frac{1}{q_\infty A_{ref} L_{ref}} \, q_\infty 2r^2 \int_0^{\pi/2} \cos^2(\varphi-\alpha) \, \sin\varphi \, (1-\cos\varphi) \, d\varphi \\
&= -\frac{1}{q_\infty A_{ref} L_{ref}} \, q_\infty 2r^2 \left(\frac{1}{12} + \sin\alpha \left(\cos\alpha \left(\frac{2}{3} - \frac{\pi}{8} \right) + \frac{1}{3}\sin\alpha \right) \right),
\end{aligned}
$$

$$
\begin{aligned}
C_m|_o^{z,circ} &= -\frac{1}{q_\infty A_{ref} L_{ref}} \, q_\infty 2r^2 \int_0^{\pi/2} \cos^2(\varphi-\alpha) \, \cos\varphi \, (-\sin\varphi) \, d\varphi \\
&= -\frac{1}{q_\infty A_{ref} L_{ref}} \, q_\infty 2r^2 \left(\frac{1}{4} + \frac{\pi}{8}\cos\alpha\sin\alpha \right),
\end{aligned}
$$

$$
z_{cp}|^{circ} = L_{ref} \frac{C_m|_o^{z,circ}}{C_x|^{circ}} = -3r \frac{\frac{1}{4} + \frac{\pi}{8}\cos\alpha\sin\alpha}{1 + \cos\alpha \, (\cos\alpha + 2\sin\alpha)},
$$

$$
x_{cp}|^{circ} = -L_{ref} \frac{C_m|_o^{x,circ}}{C_z|^{circ}} = 3r \frac{\frac{1}{12} + \sin\alpha \left(\cos\alpha \left(\frac{2}{3} - \frac{\pi}{8} \right) + \frac{1}{3}\sin\alpha \right)}{1 + \sin\alpha \, (\sin\alpha + 2\cos\alpha)}.
$$

For the complete contour we have

$$
\begin{aligned}
F_x|^{complete} &= F_x|^{circ}, \\
F_z|^{complete} &= F_z|^{circ} + 4r\sin^2\alpha, \\
C_m|_o^{x,complete} &= C_m|_o^{x,circ} - 8r^2\sin^2\alpha, \\
C_m|_o^{z,complete} &= C_m|_o^{z,circ}, \\
z_{cp}|^{complete} &= z_{cp}|^{circ}, \\
x_{cp}|^{complete} &= 3r \frac{\frac{1}{12} + \sin\alpha\cos\alpha \left(\frac{2}{3} - \frac{\pi}{8} \right) + \frac{13}{3}\sin^2\alpha}{1 + 7\sin^2\alpha + 2\sin\alpha\cos\alpha}.
\end{aligned}
$$

11.5 Problems of Chapter 6

Problem 6.1

The viscosities and the Chapman–Rubesin constant are $\mu_w = 1.88 \cdot 10^{-5}$ kg/(m s), $\mu_1 = 0.62 \cdot 10^{-5}$ kg/(m s), $C_1 = 0.9$, Reynolds number and hypersonic viscous interaction parameter are $Re_{1,l_{onset}} = 1.037 \cdot 10^5$, $\chi_1 = 8.3$, and finally the incipient separation angle is $\theta_{is} = 16.3°$.

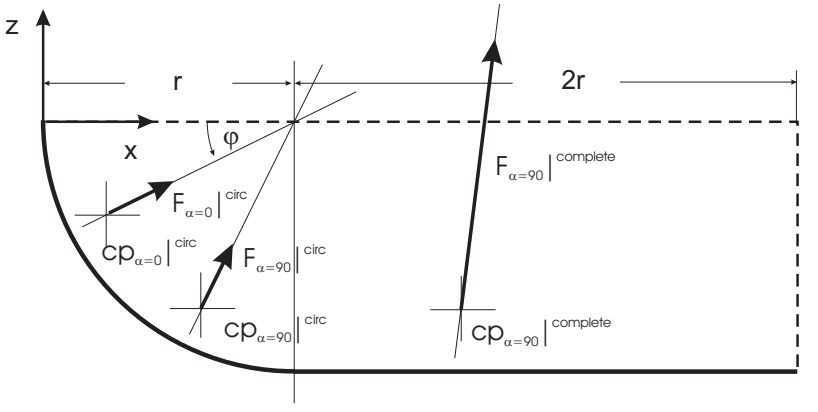

Fig. 11.1. Positions of center-of-pressure, as well as directions and magnitude of aerodynamic force vectors on the generic contour for $\alpha = 0°$ and $90°$.

Problem 6.2

Because $M_1 \gtrapprox 4.5$ we obtain $p_{2,is}/p_1 = 43.9$. From the relations for the pressure jump across an oblique shock and for the connection of shock angle θ and ramp angle $\delta \equiv \varphi$ [2]

$$\frac{p_2}{p_1} = \frac{2\gamma M_1^2 \sin^2\theta - (\gamma - 1)}{\gamma + 1},$$

and

$$\tan\delta = \frac{2\cot\theta(M_1^2 \sin^2\theta - 1)}{2 + M_1^2(\gamma + 1 - 2\sin^2\theta)},$$

we obtain $\theta = 41.8°$ and $\varphi_{is} = 32.1°$.

Problem 6.3

The pressure coefficient is:

$$c_{p_2} = \frac{p_2 - p_1}{q_1}.$$

From it we get with $p_1/q_1 = 0.5\gamma M_1^2$

$$\frac{p_2 - p_1}{p_1} = c_{p_2}\frac{\gamma}{2}M_1^2,$$

and with eq. (6.9) finally

$$\frac{p_2 - p_1}{p_1} = \frac{\gamma(\gamma + 1)}{2}M_1^2\eta^2.$$

Problem 6.4

Because $p_2/p_1 = 1$ at $\eta = 0°$ in both figures, we write

$$\frac{p_2}{p_1} - 1 = \frac{p_2 - p_1}{p_1} = \Delta\left(\frac{p_2}{p_1}\right) = C\,\eta^2.$$

a) In Fig. 6.13 we find $p_2/p_1 \approx 1.3$ at $\eta = 5°$, and with η in radians $C = 39.4$. Applying this we see that despite the small Mach number $M_{e,onset} = 2$, a reasonable agreement can be found in the interval $0° \leqq \eta \lessapprox 7°$.

b) In Fig. 6.17 we find $p_2/p_1 \approx 3$ at $\eta = 5°$, and with η in radian measure $C = 262.6$. Applying this we see that with the larger Mach number $M_{e,onset} = 10$ a reasonable agreement can be found in the somewhat larger interval $0° \leqq \eta \lessapprox 10°$.

Problem 6.5

From $\log(p/p_0) \approx -1.8$, we get $p/p_0 = p/p_\infty = 0.0158$ and with

$$c_p = \frac{2}{\gamma M_\infty^2}\left(\frac{p}{p_\infty} - 1\right),$$

and $M_\infty = 15$, $\gamma = 1.4$, finally $c_p = -0.00625$.

The vacuum pressure coefficient is $c_{p_{vac}} = -0.00635$. The base pressure is close to vacuum.

11.6 Problems of Chapter 7

Problem 7.1

1. $C_D = 1.140$, $C_L = 0.404$.
2. With eq. (7.2) we have, with the subscript 0 denoting the original data, and 1 the ones after the shift

   $$L_{ref}\,C_{m(1)} = L_{ref}\,C_{m(0)} + (x_{ref(1)} - x_{ref(0)})\,C_z - (z_{ref(1)} - z_{ref(0)})\,C_x,$$

   and $C_{m(1)} = -0.07756$.
3. The z_{ref} shift in positive direction leads always to a pitch down increment. The effect on the pitching moment of a positive x_{ref} shift depends on the sign of C_Z, which can be either positive or negative. In this case C_Z is slightly negative, so that the pitching moment experiences a small pitch down increment. Note, that $L_{ref} \equiv D_1$.

11.7 Problems of Chapter 8

Problem 8.1

Euler's equation along streamlines reads

$$VdV + \frac{dp}{\rho} = 0, \tag{1}$$

with $V^2 = u^2 + v^2 + w^2$ being the resultant velocity along a streamline. Since the inviscid flow along streamlines behaves isentropic (in flow fields without shocks), we use the thermodynamic relation for an isentropic process of a perfect gas:

$$\frac{p}{\rho^\gamma} = \text{const.} \tag{2}$$

Substitution of eq. (2) in eq. (1) and integration leads to

$$\frac{1}{2}V^2 + \frac{\gamma}{\gamma - 1}\frac{p}{\rho} = \text{const.},$$

or with $p = \rho RT$ to

$$\frac{1}{2}V^2 + c_pT = c_pT_o = \text{const.},$$

where T_o is the total temperature.

The maximum velocity is then reached for $T \longrightarrow 0$. With $c_p = \dfrac{\gamma}{\gamma - 1}R$ and $R = 287.06\ \mathrm{m^2/s^2K}$ we find [2]

$$V_{max} = \sqrt{2c_pT_o} = 1736.12\ \frac{\mathrm{m}}{\mathrm{s}}.$$

Problem 8.2

The first component of the unsteady, two-dimensional inviscid part of eq. (8.2) has the form

$$\frac{\partial}{\partial\tau}\left(J^{-1}\rho\right) + \frac{\partial}{\partial\xi}\left(J^{-1}\rho(\xi_t + \xi_x u + \xi_y v)\right) + \frac{\partial}{\partial\eta}\left(J^{-1}\rho(\eta_t + \eta_x u + \eta_y v)\right) = 0, \tag{1}$$

and of eq. (8.8)

$$\frac{\partial}{\partial t}\left(J^{-1}\rho\right) + J^{-1}\frac{\partial}{\partial x}(\rho(u - x_\tau)) + J^{-1}\frac{\partial}{\partial y}(\rho(v - y_\tau)) = 0. \tag{2}$$

The first terms of both equations are identical, so that we have to consider in each case only the second and the third terms.

From the geometrical Jacobian matrix $\mathbf{J} = \dfrac{\partial(\xi, \eta, \tau)}{\partial(x, y, t)}$ and its inverse $\mathbf{J^{-1}} = \dfrac{\partial(x, y, t)}{\partial(\xi, \eta, \tau)}$ we find for the components:

$$\xi_x = \frac{1}{J^{-1}}\, y_\eta, \qquad \xi_y = -\frac{1}{J^{-1}}\, x_\eta, \qquad \xi_\tau = \frac{1}{J^{-1}}(y_\tau x_\eta - x_\tau y_\eta),$$
$$\eta_x = -\frac{1}{J^{-1}}\, y_\xi, \qquad \eta_y = \frac{1}{J^{-1}}\, x_\xi, \qquad \eta_\tau = \frac{1}{J^{-1}}(x_\tau y_\xi - y_\tau x_\xi),$$

with the determinant $J^{-1} = x_\xi y_\eta - y_\xi x_\eta$.

Inserting these relations in eq. (1) and using the chain rules $\dfrac{\partial}{\partial x} = \xi_x \dfrac{\partial}{\partial \xi} + + \eta_x \dfrac{\partial}{\partial \eta}$, $\dfrac{\partial}{\partial y} = \xi_y \dfrac{\partial}{\partial \xi} + \eta_y \dfrac{\partial}{\partial \eta}$ in eq. (2), confirms that the identities of eq. (1) and eq. (2) are valid, if $\dfrac{\partial^2 x}{\partial \xi \partial \eta} = \dfrac{\partial^2 x}{\partial \eta \partial \xi}$ etc.

Problem 8.3

We write:

$$T_{ra} = C\, R^{-0.125},$$

and find with the value $T_w = T_{ra} = 1,490$ K from Fig. 8.18 for the radius $R = 64$ mm the constant to be $C = 2,505.87$ K/mm$^{-0.125}$. We determine with that the radiation-adiabatic temperatures for some nose radii: a) $R = 32$ mm $\Rightarrow T_{ra} = 1,624.8$ K, b) $R = 16$ mm $\Rightarrow T_{ra} = 1,771.9$ K, c) $R = 4$ mm $\Rightarrow T_{ra} = 2,107.2$ K. In Fig. 8.18, we read for these radii approximately a) $T_w = 1,585$ K, b) $T_w = 1,650$ K, c) $T_w = 1,680$ K. Our conclusion is: the smaller the nose radius, the stronger the tangential heat flux away from the nose point and the stronger the reduction of the wall temperature, which then is no more the radiation-adiabatic temperature.

Problem 8.4

The cowl lip of the inlet: due to the small lip radius!

The nozzle expansion surface: the combustion gases radiate heat towards the nozzle expansion surface (SERN) and prevent partly the cooling heat radiation away from that surface!

References

1. Schwartz, M.: New Materials, Processes, and Methods Technology. Taylor and Francis, Boca Raton (2006)
2. Hirschel, E.H.: Basics of Aerothermodynamics. Progress in Astronautics and Aeronautics, AIAA, Reston, Va, vol. 204. Springer, Heidelberg (2004)